# The Effects of Casting Methods on the Microstructure and Properties of Mg-4Al-4Ce-1Y Alloy

# HU Yong<sup>1,2</sup>, \*, WANG Ya-peng<sup>1,2</sup>, FU Ya-dong<sup>1,2</sup>, CHEN Chen<sup>1,2</sup>

- (1. School of Materials Science and Engineering, Taiyuan University of Science and Technology, Taiyuan 030024, China;
  - 2. Shanxi Key Laboratory of Copper-Based New Materials, Shanxi North Copper New Material Technology Co.,
    - 3. Ltd, Yuncheng 044000, China)

**Abstract:** This article investigates the microstructure and mechanical properties of Mg-4Al-4Ce-1Y alloy prepared by gravity casting and squeeze casting methods. The results indicate that the phase composition of the alloys prepared by the two casting methods is identical, consisting of an α-Mg matrix, a needle-like Al<sub>11</sub>(Ce,Y)<sub>3</sub> phase, a block-like Al<sub>2</sub>(Ce,Y) phase and a minor of Mg<sub>17</sub>Al<sub>12</sub> phase. However, the squeeze casting microstructure exhibits a significant grain refinement, which can significantly improve the mechanical properties of Mg-4Al-4Ce-1Y alloy. The compressive strength, yield strength, and hardness of the squeeze cast alloy reach 333.7 MPa, 117.7 MPa, and 79.7 HV, respectively, which are 19.3%, 66.7%, and 8.7% higher than those of the gravity cast alloy. However, grain refinement leads to grain boundaries impeding the free movement of electrons and phonons, thereby reducing their mean free path. As a result, the thermal diffusivity and thermal conductivity of the squeeze cast Mg-4Al-4Ce-1Y alloy are lower than those of the gravity cast alloy.

**Key words:** magnesium alloy; gravity casting; squeeze casting; microstructure; mechanical properties; thermal conductivity properties

# 1 Introduction

Magnesium alloys, featuring high specific strength, low density, and good workability, have become important lightweight structural materials. The addition of rare earth elements cerium (Ce) and yttrium (Y) can improve the heat resistance and corrosion resistance of magnesium alloys. Moreover, it can enhance the strength and hardness of magnesium alloys to a certain extent, thus meeting the requirements for high - strength and lightweight alloys in some fields [1-5]. Therefore, magnesium alloys have broad application prospects in the automotive, aerospace, 3C and other fields [6-12]. In industrial applications, magnesium alloys have attracted much attention due to their excellent properties, among which the Mg-Al-RE alloy system is an important alloy system [13,14]. Cerium is a commonly used rare earth element with a relatively low cost, which meets the requirements of low cost in alloy design. The electronegativities of cerium (Ce), aluminum (Al) and magnesium (Mg) are 1.12, 1.61 and 1.31 respectively. Since the electronegativity difference between cerium (Ce) and aluminum (Al) is the largest, the intermetallic phase of Al-Ce will be preferentially formed, thus

inhibiting the formation of Mg<sub>17</sub>Al<sub>12</sub>. Due to the relatively high melting point of the Al-Ce phase, it can act as a strengthening phase in the alloy, enhancing the mechanical properties of the material <sup>[15]</sup>, and the addition of the Y element has a similar effect. Based on the above reasons, the addition of rare earth elements plays an important role in strengthening the mechanical properties of alloys <sup>[16]</sup>.

Traditional casting processes generally suffer from numerous casting defects. In contrast, the squeeze casting process has the following characteristics compared with traditional casting processes: (1) By applying pressure, it can increase the solidification rate of the alloy, enhance the nucleation rate, and slow down the grain growth rate, thus refining the grain structure of the alloy. (2) The applied pressure helps to increase the solid solubility of solute elements. The uniformly distributed non-metallic inclusions can reduce the degree of segregation, minimize the formation of defects such as pores and shrinkage cavities, and improve the quality of the material [9]. (3) It can reduce waste and secondary processing, lower the environmental impact, and promote sustainable development [17,18]. The

squeeze casting process can effectively improve the material properties, enhance the production efficiency of alloys, reduce the production cost, and is suitable for the production needs of various industrial fields.

# 2 Materials and Methods

The Mg blocks with a purity of 99.99%, Al blocks, Mg-30%Ce master alloy and Mg-20%Y master alloy were melted in a high-frequency vacuum induction melting furnace. The Mg-4Al-4Ce-1Y alloy samples for gravity casting were prepared by induction melting in a graphite crucible at a melting temperature of 750 °C, followed by furnace cooling. The size of the samples is  $\Phi$ 20×100 mm. The extrusion device consists mainly of a quartz tube, a push rod and a copper mold [19]. The extrusion device was installed in the high-frequency vacuum induction melting furnace, and the alloy was melted in the quartz tube. After the sample was melted, the molten alloy was injected into the copper mold by driving the push rod with an air pump. The extrusion speed is 0.3 m/s, and the cooling rate of the copper mold is about 200 K/s. The rod-shaped samples with a size of  $\Phi$ 8 mm were obtained after squeeze casting.

The squeeze casting samples were cut into cylindrical specimens with a diameter of Φ6 mm. These cylindrical specimens were inlaid, then polished with silicon carbide sandpapers ranging from 120 to 2000 mesh, and subsequently polished with a 0.5 µm diamond polishing paste. The specimens were etched with a 4% nitric acid-alcohol solution. The microstructure was observed and energy-dispersive spectroscopy (EDS) analysis was carried out using a scanning electron microscope (SEM) JSM-6510) and an energy-dispersive spectrometer X-200 (EDS) (OXFORD max). The composition of the samples was analyzed by X-ray diffraction (XRD) (Empyrean from the Netherlands) with a Cu target using the Cu-K $\alpha$  line, and the scanning range was from 5° to 90°.

The compression properties were tested on a universal testing machine (CTM-4304). The indenter speed was 0.2 mm/min, and the size of the compression specimen was  $\Phi6\times10$  mm. The fracture morphology of the specimens was observed by scanning electron microscopy (SEM).

# 3 Experiment results

#### 3.1 Microstructure

The metallographic structures the Mg-4Al-4Ce-1Y alloy prepared by gravity casting and squeeze casting are shown in Fig. 1. Fig. 1 (a) corresponds to the as-cast alloy structure. A large number of fine blocky or strip-shaped phases can be observed to aggregate, and under the metallographic microscope, the second phase appears as dark agglomerated shapes. Fig. 1 (b) and (c) correspond to the metallographic photos of the squeeze casting Mg-4Al-4Ce-1Y alloy at magnifications of 200 times and 500 times. It can be seen that after squeeze casting, the agglomerated and disorderly distributed second phase transforms into a dendritic structure, and the number of the second phase increases. The grain boundaries of the sample are very obvious. Under fast cooling conditions, when liquid alloys are crystallized in a dendritic manner, due to the slow diffusion of atoms in the solid phase to a uniform process, the dendrites first precipitated, the dendrites later precipitated, and the dendritic interstitial have different compositions. The first precipitated dendrites contain more high-melting point components, while the dendritic interstitial contains more low-melting point components.

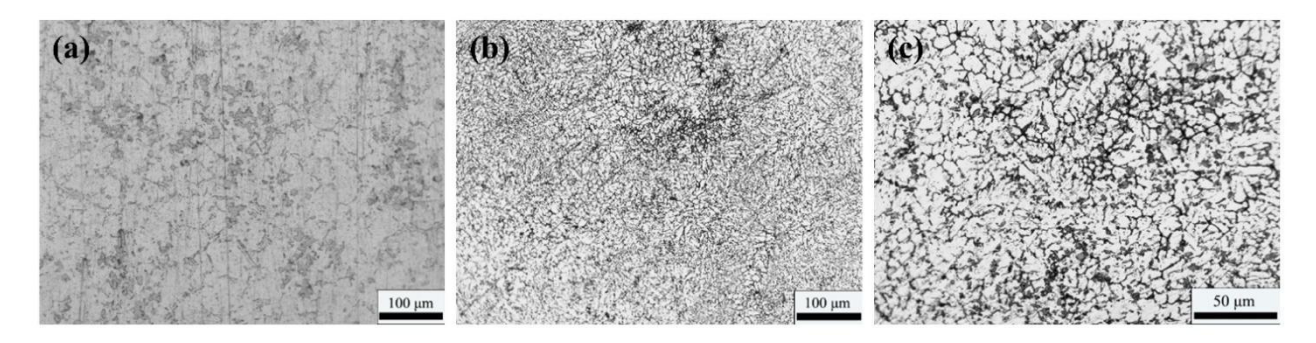


Fig 1. Metallographic photos of Mg-4Al-4Ce-1Y alloy produced by gravity casting and squeeze casting:

(a) gravity casting (b) squeeze casting×200 (c) squeeze casting×500

Due to the use of copper molds in extrusion casting, the cooling rate is faster. With a relatively fast cooling rate, atoms of Al, Ce and Y in the metal do not have enough time to diffuse and migrate. Affected by the grain boundary energy, they will accumulate at the grain boundaries. According to the Gibbs-Thomson equation, the nucleation rate is proportional to the supersaturation. As the solidification temperature decreases, the solubility of Al, Ce and Y atoms decreases, making the alloy more likely to be supersaturated, thus increasing the nucleation rate and slowing down the grain growth rate [20]. The solidification theory indicates that the nucleation rate I and the growth rate V determine the grain size of the solidified alloy. However, both the nucleation rate and the growth rate are related to the cooling rate, and the

magnitudes of their accelerations are different. The quantitative relationship between them and the grain size d can be expressed as <sup>[21]</sup>:

$$d = \left(\frac{V}{I}\right)^{\frac{1}{4}} \tag{1}$$

The grain size decreases with an increase in the nucleation rate and increases with an increase in the growth rate. When the cooling rate is fast, the undercooling degree becomes larger, the free energy difference between the liquid phase and the solid phase becomes larger, the crystallization driving force becomes larger, and the growth rate of the nucleation rate is greater than the growth rate. Therefore, the higher the cooling rate, the smaller the ratio *V/I* and the finer the grain.

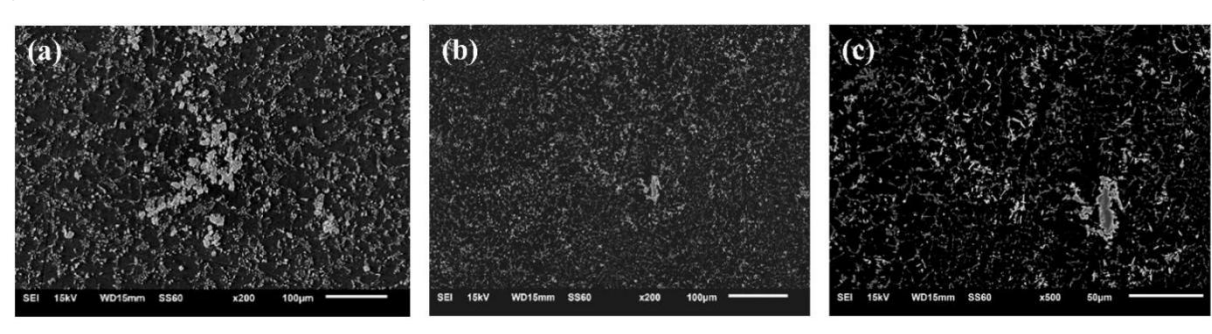
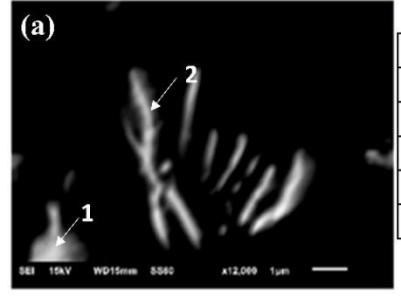


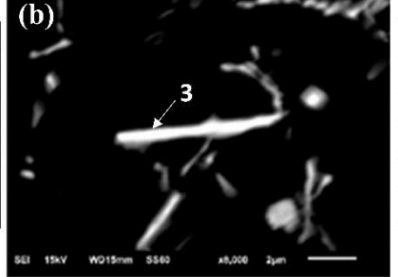
Fig 2. SEM photos of Mg-4Al-4Ce-1Y alloy fabricated by gravity casting and squeeze casting:
(a) gravity casting (b) squeeze casting×200 (c) squeeze casting×500

Fig. 2 and 3 show the scanning electron microscopy (SEM) photos and the results of energy-dispersive spectroscopy (EDS) analysis of the Mg-4Al-4Ce-1Y alloy prepared by gravity casting and squeeze casting. According to the atomic ratios obtained by EDS, the network structure consists of Al<sub>11</sub>(Ce,Y)<sub>3</sub>and Mg<sub>17</sub>Al<sub>12</sub>, while the agglomerated blocky phase is Al<sub>2</sub>(Ce,Y). Thus, the phase composition of Mg-4Al-4Ce-1Y includes the α-Mg matrix, Al<sub>11</sub>(Ce,Y)<sub>3</sub>, Al<sub>2</sub>(Ce,Y), and Mg<sub>17</sub>Al<sub>12</sub>. For the

squeeze casting alloy, according to the EDS analysis, the atomic percentage of Al and (Ce,Y) in the slender acicular phase is close to 11:3, indicating that the slender acicular phase is Al<sub>11</sub>(Ce,Y)<sub>3</sub>; the atomic percentage of Al and (Ce,Y) in the blocky phase is 2:1, meaning that the blocky phase is Al<sub>2</sub>(Ce,Y). In addition to the separately distributed slender acicular Al<sub>11</sub>(Ce,Y)<sub>3</sub> phase in the figure, the situation where the blocky Al<sub>2</sub>(Ce,Y) is connected to the slender acicular Al<sub>11</sub>(Ce,Y)<sub>3</sub> can also be observed.



| 谱图1 |      | 谱图2 |      |
|-----|------|-----|------|
|     | At.% |     | At.% |
| Mg  | 71.7 | Mg  | 83.5 |
| Al  | 19.1 | AI  | 13.6 |
| Ce  | 7.9  | Ce  | 2.6  |
| Υ   | 1.3  | Y   | 0.3  |



| 谱  | 谱图3  |  |
|----|------|--|
|    | At.% |  |
| Mg | 88.0 |  |
| Al | 8.1  |  |
| Ce | 3.2  |  |
| Υ  | 0.6  |  |

Fig 3. EDS photos of gravity casting and squeeze casting of Mg-4Al-4Ce-1Y alloy:

(a) squeeze casting×12000 (b) squeeze casting×9000

# 3.2 Mechanical properties

Fig. 4 shows the compression stress-strain curves at room temperature of the Mg-4Al-4Ce-1Y alloy samples prepared by gravity casting and squeeze casting. Table 1 presents the compression properties of the Mg-4Al-4Ce-1Y alloy. Compared with the gravity casting samples, the compressive strength and yield strength of the squeeze casting Mg-4Al-4Ce-1Y alloy have been significantly improved. The compressive strength has increased from 279.8 MPa to 333.7 MPa, an increase of 19.3%, and the yield strength has increased from 70.6 MPa to 117.7 MPa, an increase of 66.7%.

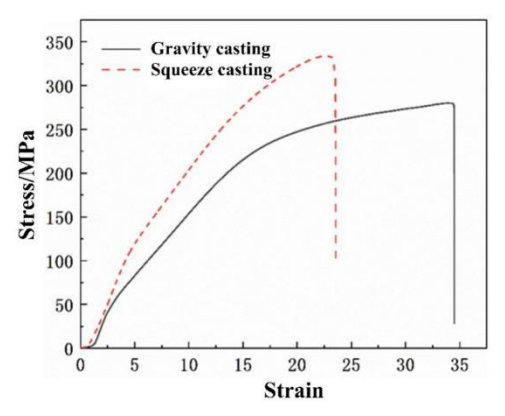


Fig 4. Stress-strain curves of gravity casting and squeeze casting of Mg-4Al-4Ce-1Y alloy

Table. 1 Compressive properties of Mg-4Al-4Ce-1Y alloy

| sample          | compressive<br>strength/MPa | yield<br>strength/M<br>Pa | deformati<br>on/% |
|-----------------|-----------------------------|---------------------------|-------------------|
| Gravity casting | 279.8                       | 70.6                      | 34.5              |
| Squeeze casting | 333.7                       | 117.7                     | 23.6              |

Table 2 shows the Vickers hardness of the Mg-4Al-4Ce-1Y alloy. As can be seen from the table, compared with gravity casting, the hardness of the squeeze casting sample has increased. The average hardness has increased from 73.3 HV to 79.7 HV, representing an increase of 8.7%.

Tab. 2 Vickers hardness comparison for Mg-4Al-4Ce-1Y alloy

| Vickers hardness/HV |      |      |      |         |
|---------------------|------|------|------|---------|
| Specimen number     | 1    | 2    | 3    | Average |
| Gravity casting     | 72.7 | 72.4 | 74.9 | 73.3    |
| Squeeze casting     | 80.3 | 79.1 | 79.7 | 79.7    |

It is widely acknowledged that the grain size is a major factor influencing the strength of an alloy. The relationship between the strength of the alloy and the grain size can be expressed by the Hall - Petch formula<sup>[22]</sup>:

$$R_{eL} = \sigma_0 + Kd^{-\frac{1}{2}} \tag{2}$$

In the formula (2),  $R_{eL}$  is the strength,  $\sigma_0$  is a constant, which is generally determined by the properties of the material itself, depending on the crystal structure and dislocation density; K is a constant, which characterizes the degree of influence of grain boundaries on the strength; d is the average diameter of each grain in a polycrystal.

Compared to gravity casting, the microstructure of the squeeze casting Mg-4Al-4Ce-1Y alloy is significantly refined. The grain size of the alloy decreases and the number of grain boundaries increases. Grain boundaries can effectively impede dislocations. As a result, dislocations accumulate near the grain boundaries, leading to local stress concentration. This, in turn, promotes the activation of dislocation sources in adjacent grains; at the same time, the finer the grain, the larger the grain boundary area, the more tortuous the grain boundaries will be, which is not conducive to the propagation of cracks, thus playing a role in fine grain strengthening [22]. However, the higher the energy near the grain boundary, the disordered arrangement of atoms, resulting in entanglement and dislocation stuffing of normal lattice slip dislocations, which in turn increases the dislocation density and leads to increased dislocation movement resistance [23]. It can be seen from formula (2) that when the grain size in the alloy decreases and the dislocation density increases, the strength of the alloy increases under the action of dislocation strengthening. Therefore, under the combined action grain strengthening of fine and dislocation strengthening, the compressive strength, yield strength and hardness of the squeeze casting samples are significantly improved than those of the gravity casting samples.

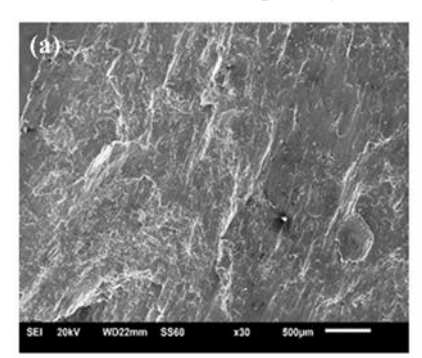
# 3.3 Fracture morphology and analysis

Fig. 5 (a) shows the fracture morphology of gravity-cast Mg-4Al-4Ce-1Y alloy. It can be seen from the figure that the dimple is torn under the action of shear stress, resulting in a flat rocky step at the fracture. There are some shallow pits on the surface of the step, and the "river" pattern is elongated,

indicating a certain local plastic deformation, which is characterized by tough and brittle mixed fracture.

Fig. 5 (b) shows the fracture morphology of

extrusion casting Mg-4Al-4Ce-1Y alloy. It can be seen from the drawing that the fracture is relatively flat, showing the characteristics of typical brittle fracture.



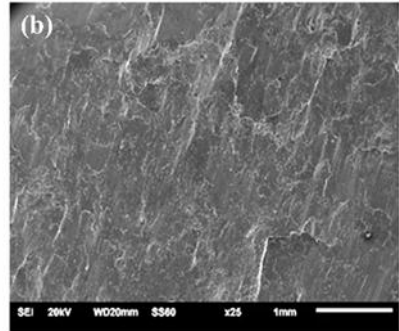


Fig 5. Fracture morphology of Mg-4Al-4Ce alloy produced by gravity casting and squeeze casting:

(a) squeeze casting×30 (b) squeeze casting×25

# 3.4 Thermal conductivity

Table 3 shows the thermal diffusion coefficients and thermal conductivity of the gravity casting and squeeze casting Mg-4Al-4Ce-1Y samples at room temperature. The thermal diffusion coefficients of the gravity cast and squeeze casting samples at room temperature were 51.9 mm<sup>2</sup>s<sup>-1</sup> and 44.1 mm<sup>2</sup>s<sup>-1</sup>, and

the thermal conductivities were 92.7 Wm<sup>-1</sup>·K<sup>-1</sup> and 78.9 Wm<sup>-1</sup>·K<sup>-1</sup>, respectively. Compared with the gravity cast samples, the thermal diffusion coefficients and thermal conductivity of the squeeze casting Mg-4Al-4Ce-1Y alloy samples were both reduced.

Table 3 The thermal conductivity of Mg-4Al-4Ce-1Y alloy

| sample          | thermal diffusion coefficient | density            | specific heat capacity | thermal conductivity   |
|-----------------|-------------------------------|--------------------|------------------------|------------------------|
|                 | $mm^2 \cdot s^{-1}$           | g·cm <sup>-3</sup> | $Jg^{-1} \cdot K^{-1}$ | $Wm^{-1} \cdot K^{-1}$ |
| gravity casting | 51.9                          | 1.803              | 0.991                  | 92.7                   |
| squeeze casting | 44.1                          | 1.803              | 0.991                  | 78.9                   |

In metals and their alloys, both electronic thermal conductivity and phonon thermal conductivity are important thermal conductivity methods, and the thermal conductivity of the material is composed of electronic thermal conductivity and phonon thermal conductivity.

$$\lambda = \lambda_e + \lambda_L \tag{3}$$

In the formula (3),  $\lambda$  is the metal thermal conductivity,  $\lambda_e$  is the electron thermal conductivity,  $\lambda_L$  is the phonon thermal conductivity.

It is well known that the existence of intermetallic phases and grain boundaries will destroy the original periodic arrangement of metal crystal lattices, increase the scattering probability of phonons and electrons during propagation, and reduce the mean free paths of phonons and electrons, thereby reducing the thermal diffusion coefficient and thermal conductivity of metals. Moreover, with the increase of the number of intermetallic phases and grain

boundaries in the matrix, the greater the impact on the thermal diffusion coefficient and thermal conductivity of metals <sup>[25]</sup>. Therefore, the thermal diffusion coefficient and thermal conductivity of squeeze casting samples are lower than those of gravity casting samples.

# **4 Conclusion**

The Mg-4Al-4Ce-1Y alloy was prepared by different casting methods (i.e. gravity casting and squeeze casting), and the following conclusions were obtained:

1.The phase compositions of Mg-4Al-4Ce-1Y alloys by gravity casting and squeeze casting are  $\alpha$ -Mg matrix, Al<sub>11</sub>(Ce, Y)<sub>3</sub>, Al<sub>2</sub>(Ce, Y) and Mg<sub>17</sub>Al<sub>12</sub>. Among them, Al<sub>11</sub>(Ce, Y)<sub>3</sub> is a slender needle-like phase, which is uniformly distributed on the grain boundary; Al<sub>2</sub>(Ce, Y) is large granular or short rod-like, and a small amount of Mg<sub>17</sub>Al<sub>12</sub> is distributed on the alloy

matrix.

- 2.The mechanical properties of extrusion-cast Mg-4Al-4Ce-1Y alloys are significantly improved compared to gravity-cast alloys. The compressive strength is increased from 279.8 MPa to 333.7 MPa, an increase of 19.3%, and the yield strength is increased from 70.6 MPa to 117.7 MPa, an increase of 66.7%. The average hardness is increased from 73.3 HV to 79.7 HV, an increase of 8.7%.
- 3. The thermal diffusion coefficients of gravity casting and squeeze casting samples at room temperature are 51.9 mm<sup>2</sup>s<sup>-1</sup> and 44.1 mm<sup>2</sup>s<sup>-1</sup>, respectively, and the thermal conductivities are 92.7 Wm<sup>-1</sup>·K<sup>-1</sup> and 78.9 Wm<sup>-1</sup>·K<sup>-1</sup>.

### References:

- [1] 刘旭贺, 刘振凯, 刘希东. 挤压变形 Mg-5Li-2.6Al-1.8Zn 合金的显微组织及力学性能[J]. 轻合金加工技术, 2023, 51 (08): 23-27.
- [3] 陈芙蓉, 李仕慧, 郭锋, 等. 铈对 AZ91D 镁合金组织和力学性能的影响[J]. 铸造技术, 2009, 30 (02): 203-206.
- [4] WU GUO-HUA, WANG CUN-LONG, SUN MING, et al. Recent developments and applications on high-performance cast magnesium rare-earth alloys[J]. Journal of Magnesium and Alloys, 2021, 9 (01): 1-20.
- [5] 李上民, 杨明波, 李春雨, 等. 稀土对 Mg-Al 镁合金组织 和性能影响研究进展[J]. 特种铸造及有色金, 2022, 42 (03): 329-336.
- [6] NAGASIVAMUNI B, WANG GUI, MARK A E, et al. A comparative study of the role of solute, potent particles and ultrasonic treatment during solidification of pure Mg, Mg–Zn and Mg–Zr alloys[J]. Journal of Magnesium and Alloys, 2021, 9 (03): 829-839.
- [7] CHEN JUN, FENG JU, YAN LEI, et al. In situ growth process of Mg–Fe layered double hydroxide conversion film on MgCa alloy[J]. Journal of Magnesium and Alloys, 2021, 9 (03): 1019-1027.
- [8] KNAPEK M, MÁRIA Z, GREŠ A, et al. Corrosion and mechanical properties of a novel biomedical WN43 magnesium alloy prepared by spark plasma sintering[J]. Journal of Magnesium and Alloys, 2021, 9 (03): 853-865.
- [9] 贾海龙, 张梦娜, 杨铭, 等. 挤压铸造镁合金研究进展 [J]. 中国材料进展, 2021, 40 (10): 772-784.
- [10] 王昊昊, 韩艳. 中南大学利用镁合金涂层打造外科医用新材料[N]. 中国科学报, 2023-12-25(003).
- [11] 杨鸿智, 尹小文, 苏彦芳, 等. 镁合金零部件在汽车中

- 的应用研究[J]. 汽车工艺师, 2023 (10): 56-59.
- [12] 刘普林,周佳膑,曹忠,等. 航天领域镁合金标准体系建设研究与实践[J]. 航天标准化,2023 (02): 30-33.
- [13] HAN GUANG, LIU XIANG-FA. Phase control and formation mechanism of Al–Mn(–Fe) intermetallic particles in Mg–Al-based alloys with FeCl<sub>3</sub> addition or melt superheating, Acta Materialia, 2016, 114: 54-66.
- [14] HAN MENG-YAN, ZHU XIANG-ZHEN, GAO TONG, et al. Revealing the roles of Al<sub>4</sub>C<sub>3</sub> and Al<sub>8</sub>Mn<sub>5</sub> during α-Mg nucleation in Mg-Al based alloys[J]. Journal of Alloys and Compounds, 2017, 705: 14-21.
- [15] 吴义邦. Mg-3Al-6RE 合金显微组织演化及力学性能研究[D]. 哈尔滨: 哈尔滨理工大学, 2021.
- [16] DARGUSCH M S, ZHU SU-MING, NIE JIAN-FENG, et al. Microstructural analysis of the improved creep resistance of a die-cast magnesium-aluminium-rare earth alloy by strontium additions[J]. Scripta Materialia, 2009, 60: 116-119.
- [17] 涂卫军, 王刚. 铝合金汽车转向节挤压铸造工艺研究 [J]. 铸造, 2015, 64 (08): 740-743.
- [18] 王伟, 崔晓明, 石博, 等. 铝合金轮毂连接盘挤压铸造数值模拟[J]. 铸造, 2021, 70 (03): 306-310.
- [19] SONG XIN, HU YONG, TIAN JIN-SONG, et al. Effects of addition of yttrium on the microstructure, compression properties and corrosion resistance of squeeze casting AZ91D-1.6Ca magnesium alloy[J]. International Journal of Metalcasting, 2024, 18: 292-302.
- [20] 田皓, 彭渝丽, 袁满, 等. 冷却速率对 Al-2Cu-5Ni 合金相组织及力学性能影响[J]. 特种铸造及有色合金, 2023, 43 (12): 1705-1709.
- [21] 吴泽光. 快冷细晶 Mg-Al-Y 合金制备及其热处理工艺研究[D]. 南昌: 南昌航空大学, 2019.
- [22] 管博. 密排六方金属细晶强化取向相关性的定量研究 [D]. 重庆; 重庆大学, 2022.
- [23] 杨伟, 殷海眯, 聂海明, 等. 含 SiC 颗粒亚快速凝固镁 合金的组织与性能[J]. 稀有金属材料与工程, 2017, 46 (10): 3146-3150.
- [24] 崔洋, 李寿航, 应韬, 等. 基于第一性原理的金属导热性能研究[J]. 金属学报, 2021, 57 (03): 375-384.
- [25] 苏创业. 基于固溶原子和第二相的镁合金导热机制研究[D]. 上海: 上海交通大学, 2020.